Lasers in Medical Science (2019) 34:1243–1251
https://doi.org/10.1007/s10103-019-02720-9

ORIGINAL ARTICLE

In vivo detection of oral precancer using a fluorescence-based, in-house-fabricated device: a Mahalanobis distance-based classification

Pavan Kumar[1] · Surendra Kumar Kanaujia[2] · Ashutosh Singh[2] · Asima Pradhan[1,3]

Received: 13 July 2018 / Accepted: 10 January 2019 / Published online: 19 January 2019
© Springer-Verlag London Ltd., part of Springer Nature 2019

Abstract

In vivo detection of oral precancer has been carried out by a fluorescence-based, in-house-developed handheld probe on three groups: oral squamous cell carcinoma (OSCC), dysplastic (precancer), and control (normal). Measurements have been performed on a total of 141 patients and volunteers of different age groups. Excitation wavelength of 405 nm was used and fluorescence emission spectra were recorded in the scan range of 450.14 to 763.41 nm at very low incident power (122 μW) from different oral sites buccal mucosa (BM), lateral boarder of tongue (LBT), and dorsal surface of tongue (DST). Spectral profiles are found to vary among the three groups as well as among the different oral sites. Major and minor bands of flavin adenine dinucleotide (FAD) and porphyrins near 500, 634, 676, 689, and 703 nm have been obtained. Porphyrin contribution is found to be more dominant than the FAD in OSCC and dysplastic groups as compared to the control group. A better classification has been observed using the entire spectral range rather than restricting to individual bands, by application of principal component analysis (PCA), Mahalanobis distance model, and receiver operating characteristic analysis (ROC). ROC on Mahalanobis distance differentiates OSCC to normal, dysplastic to normal, and OSCC to dysplastic with sensitivities from 71% to 98%, 92% to 94% and 81% to 93% and specificities 91% to 100%, 86% to 100% and 79% to 97% for oral sites BM, LBT and DST. LBT and DST appear to be more sensitive to dysplasia detection as compared to BM.

Keywords Oral cancer · Oral sites · Fluorescence spectroscopy · Principle component analysis · Mahalanobis distance model · Receiver operating characteristic analysis

Introduction

Worldwide, oral cancer is the 6th most common malignancy and according to survey, it is predicted that incidence rate of oral cancer in India will be more than 1.7 million in 2035 from 1 million in 2012. It is pertinent to note that the northern region of India has a huge population addicted to tobacco and pan masala, which makes them vulnerable to various problems of the oral cavity. A 5-year survival rate with diagnosis at advanced stage is less than 50% and has not improved in the past decades. Poor survival rate is higher due to late diagnosis and lack of early symptoms. There is a higher chance of cure for oral cancer by early detection and therefore possible to reduce the morbidity and mortality rate. Oral premalignant lesion starts in the form of leukoplakia, erythroplakia, erythroleukoplakia, and oral submucosal fibrosis (OSMF) and converts into malignancy (squamous cell carcinoma) with different rates [1–6].

Among the various fluorophore molecules present in the human tissue, the major ones are tryptophan, collagen, nicotinamide adenine dinucleotide (NADH), flavin adenine dinucleotide (FAD), and porphyrins. It has been established that during the progression of disease, concentrations of fluorophores change due to the increased tissue metabolic activity. Studies reveal that contribution of NADH increases as the disease progresses and FAD contribution decreases while porphyrin contribution shows enhancement. Porphyrins occur in various forms such as uroporphyrin, zinc protoporphyrin IX (ZnPP), coproporphyrin (CP), and protoporphyrin IX (PpIX). It gives orange (590–620 nm) to red (620–750 nm) fluorescence.

✉ Asima Pradhan
asima@iitk.ac.in

[1] Department of Physics, Indian Institute of Technology Kanpur (IITK), Kanpur 208016, India

[2] Department of ENT, Ganesh Shankar Vidyarthi Memorial College (GSVM), Kanpur 208002, India

[3] Center for Lasers and Photonics (CELP), IIT Kanpur, Kanpur 208016, India

Porphyrins, in particular PpIX, are found in cancerous as well as healthy tissues, saliva, blood, etc. and its accumulation increases with the progress of cancer [7–9].

Conventional biopsy techniques used for identifying oral premalignant and malignant lesions are visual inspection, use of toluidine blue, brush biopsy, and tissue biopsy by pathologist, among which tissue biopsy with histopathology is most reliable. Tissue biopsy is an invasive procedure with the complication of inability to select best area for biopsy, since the lesions are spread over a large area of oral cavity [1, 6]. Different noninvasive techniques such as fluorescence spectroscopy, Raman spectroscopy, diffuse reflectance spectroscopy, and Stokes shift spectroscopy have been extensively used for in vivo and in vitro study to differentiate premalignant and malignant lesions for different cancers. Among these techniques fluorescence spectroscopy is widely used by several researches for oral cancer detection as an in vivo study and has been established as a good diagnostic tool [10–19]. Properties such as high sensitivity, less time consumption, and its noninvasive nature make it a potential candidate for in vivo detection of cancer. Attempts have been made to detect oral cancer through different body fluids such as saliva, blood, and urine. This has shown great potential in discriminating the oral lesions [20–22]. Our group has also showed saliva for early detection of oral cancer [23]. Inaguma M. and Hashimoto K. have found that 85% of carcinomas show porphyrin-like fluorescence by using in-house-developed NEAD system [9]. Gillenwater et al. had studied oral neoplasia and observed that the ratio of the red to blue intensities were greater in abnormal tissue. They achieved sensitivity of 88% and specificity of 100% in differentiating abnormal to normal mucosa [24]. A pilot study was performed by Majumder et al. using fluorescence spectroscopy and they were able to differentiate cancer to normal oral mucosa with 86% sensitivity and 63% specificity [25]. Handheld device was used for visualization of oral-cavity tissue fluorescence by Lane et al. for early cancer detection. A sensitivity and specificity of 98% and 100% was achieved on differentiating normal mucosa from sever dysplasia and invasive carcinoma [26]. Diana C.G. de Veld performed an anatomy-based study of healthy oral mucosa and observed differences in fluorescence intensity in oral mucosal sites [27]. Jayanthi et al. had employed principal component analysis (PCA) and LDA on fluorescence and diffuse reflectance data of oral lesion and were able to differentiate the lesions with AUC-ROC values of 0.987 for fluorescence and 0.991 for diffuse reflectance spectroscopy [28]. Nazeer et al. group achieved a sensitivity of 60 to 100% and specificity of 76 to 100% in discriminating oral lesions using fluorescence spectroscopy [29].

In this study, we report in vivo detection of oral cancer as well as precancer based on fluorescence from FAD and porphyrin using excitation source of 405 nm. An in-house-developed handheld probe is able to detect fluorescence signal at very low power incident on the oral mucosa [28]. Site (anatomy)-based classification has been performed due to differences in spectral profile in different oral anatomical locations (buccal mucosa, tongue, soft and hard palate, etc.). Porphyrin fluorescence is found to be very common in OSCC and dysplastic groups than the control. As per our knowledge, ROC on Mahalanobis distance has not been employed for oral precancer classification. Site-based classification done by research groups are also limited. Multivariate analysis (PCA, Mahalanobis distance model, and ROC) performed in the spectral ranges (451–590 nm) and (591–763 nm) separately have shown good discrimination among the groups (OSCC, dysplastic, and control) in the spectral range (591–763 nm) due to dominance of porphyrin bands over the FAD band, while an even better discrimination has been achieved in the entire spectral range (451–763 nm), since in few cases FAD dominant over porphyrin.

Materials and methods

Instrumentation and data collection

Measurements were performed on 166 tissue sites of 67 OSCC patients, 126 tissue sites of 38 dysplastic patients and 160 tissue sites of 36 normal volunteers of different age groups. Patients reporting to clinicians for treatment were asked not to consume food and beverage and to clean their oral cavity with water. It was noticed that most patients reporting in hospital had some common habits such as tobacco and pan masala chewing and occasional consumption of alcohol. Out of the 105 patients, 83 were male and 22 female. The age of patients (OSCC/dysplastic) and normal volunteers are

Table 1 Training and validation data sets for all the sites (BM, LBT, and DST) for Mahalanobis distance calculation

Patient/ volunteers	PC scores of BM		PC scores of LBT		PC scores of DST	
	Training data set	Validation data set	Training data set	Validation data set	Training data set	Validation data set
OSCC	40	39	28	27	16	16
Dysplasia	24	24	25	24	15	14
Normal	31	31	30	30	19	19

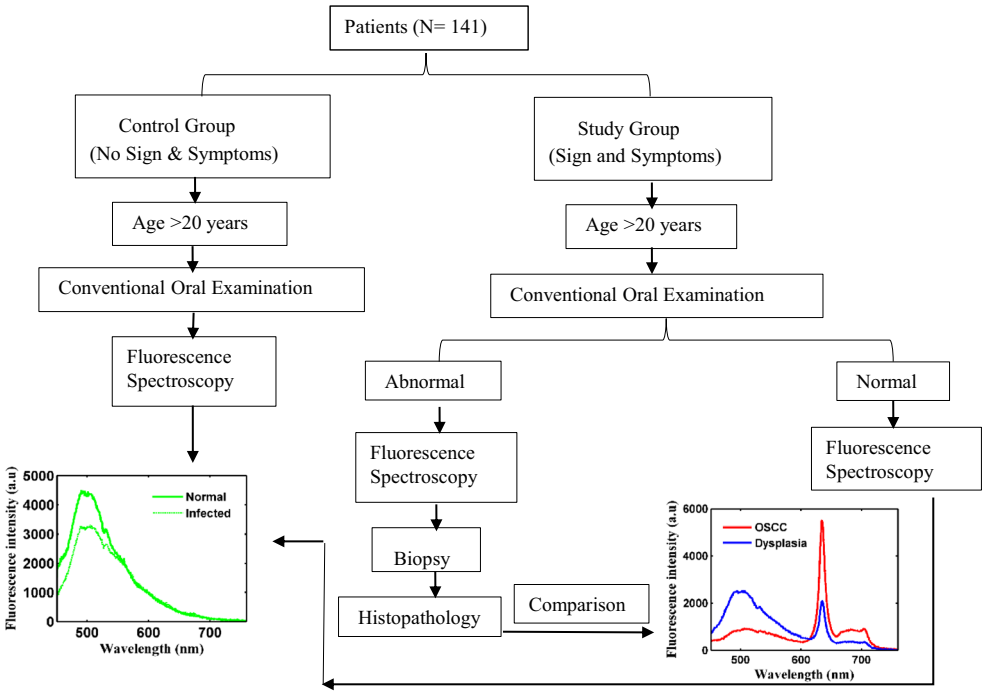

Fig. 1 In vivo study protocol of inclusion and exclusion of patients

listed in Table 1. Study protocol for the inclusion and exclusion of the patients is shown in Fig. 1. In the control group, volunteers were restricted to only those free from any disease and habits. In the abnormal group, patients with symptoms (whitish, reddish patches, and raised growth) were included. Few of the abnormal patients who displayed some signs due to infection were excluded from the abnormal group after taking fluorescence data. The outcome of such patients was found to be similar to the control group. Finally comparison of fluorescence data with histopathology was done and used for further analysis.

Follow-up of ethical approval

Ethical clearance was obtained with IEC communication number IITK/IEC/2015-16/2/10 and clinical trials registry-India (CTRI) was also approved with registration number CTRI/2017/10/010102. All participating patients and volunteers were explained about the procedure and informed consent was taken before the testing. All the details of patients such as age, occupation, family background, life style, habits (especially cigarette/bidi smoking, alcohol consumption, etc.) were noted in a questionnaire.

Fluorescence measurements were taken with a handheld device which was fabricated in-house (CELT workshop, IIT Kanpur, India) and installed in Hallet Hospital, affiliated to GSVM Medical College Kanpur. The block diagram and photograph of the device are shown in Fig. 2a and b respectively. The probe consists of optical components such as collimating lens (CL) and beam splitter (BS) and connecting fibers. Laser light from a fiber-coupled 405-nm diode laser (Diode Laser 405 nm, Model: ADR-1805, Pegasus Shanghai Optical System Co. Ltd., Shanghai China) fell on the beam splitter (UVFS Plate Beamsplitter, Model: BSS10R, 25 × 36 nm 30:70 (R:T), Newton, NJ, USA) after passing through a collimating lens (74-series Collimating Lenses, 200–2000 nm, Ocean Optics, FL, USA). Reflected part of light falls on the tissue of oral cavity via a focusing lens (Achromatic Doublets, AR Coated: 400–700 nm,

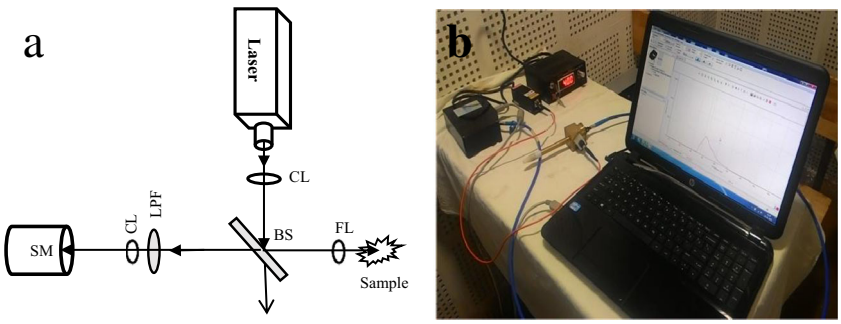

Fig. 2 **a** In-house-fabricated handheld device for oral cancer detection: 405-nm laser diode (LD), collimating lens (CL), beam splitter (BM), focusing lens (FL), long pass filter (LPF), spectrometer (SM). Fig. 1 **b** photograph of handheld unit with other required components

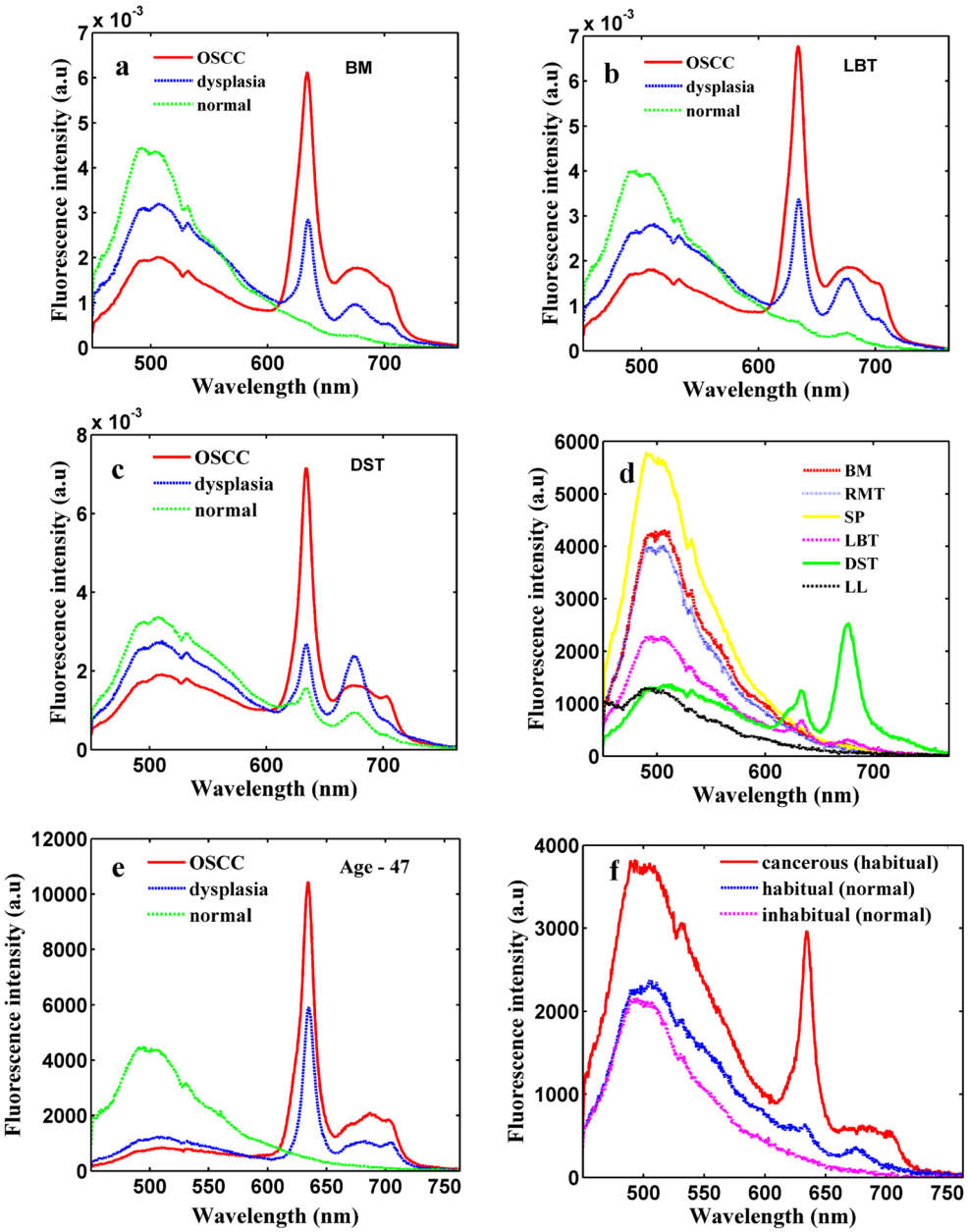

Fig. 3 Area normalized averaged fluorescence spectra for OSCC, dysplastic, and normal oral mucosa at excitation wavelength 405 nm in the scan range 450.14–763.41 nm recorded from **a** BM, **b** LBT, **c** DST, **d** typical spectra of oral sites (BM, RMT, SP, LBT, DST, and LL) from a control group, **e** typical spectra of 47 years old OSCC and dysplastic patients and a volunteer, and **f** typical spectra of OSCC, habitual, and inhabitual patients

Thorlabs, Newton, NJ, USA). Fluorescence signal produced by the oral tissue is transmitted through beam splitter and recorded by a fiber coupled spectrometer (HR 2000$^+$, Ocean Optics, Inc., FL, USA) by a collimating lens. A 450-nm long pass filter (Longpass Filter, Model: FEL0450, Thorlabs, Newton, NJ, USA) was used to avoid specular reflection. The spectrometer is interfaced with the laptop (Sony Vaio E Series, Intel Core i5-2450M, 2.50GHz, 4GB RAM, 64-bit Windows 10 Operating System, Japan) via its USB port. Ocean Optics Spectra Suit Software (Ocean Optics, FL, USA) has been used for acquisition. A removable disposable cap of Teflon material (Virgin PTFE, HINDUSTAN NYLONS, Maharashtra, India) is inserted at the tip of the probe. An optimal power of 122 μW falling on the oral cavities of patients and volunteers was sufficient to produce measurable fluorescence. Different sites (buccal mucosa, tongue, lip, soft and hard palate, etc.) of oral cavity were irradiated with laser light with 3-s integration time and recorded in the scan range of 450.14 to 763.41 nm at the interval of 0.46 nm.

Analysis methods

Recorded data sets are higher dimensional (681) and are reduced through PCA to capture maximum information. Data sets of fluorescence spectra (681) are reduced into a

Table 2 Number of patients (OSCC/dysplastic) and volunteers with their mean age and standard deviation (SD) and number of measured sites from buccal mucosa (BM), lateral boarder of tongue (LBT), and dorsal surface of tongue (DST)

Patients/volunteers	Age	Mean age with SD	BM patients (no. of sites)	LBT patients (no. of sites)	DST patients (no. of sites)
OSCC	36–73	48 ± 11	36 (79)	20 (55)	11 (32)
Dysplasia	22–61	39 ± 8	19 (48)	18 (49)	9 (29)
Normal	24–52	36 ± 7	36 (62)	36 (60)	17 (38)

lower dimension (11) by evaluating the principal components (PCs) of the correlation matrix (681 × 681). PC scores are estimated by projecting the original data along the PCs. Classification among the data sets has been done using Mahalanobis distance model by computing Mahalanobis distances for the PC scores. Data sets of PC scores are divided into training and validation sets as shown in Table 1. Mahalanobis distances (D_{maha}) of validation data sets (V) are calculated from the mean of training data set (t_m) with the help of the following equation.

$$D_{maha} = \sqrt{(V-t_m)' C_t^{-1} (V-t_m)} \quad (1)$$

where C_t^{-1} is the inverse of the covariance matrix of the training data set.

Receiver operating characteristic (ROC) is employed on the binary data sets of Mahalanobis distances to evaluate the efficacy of the test as well as to calculate diagnostic parameters [15, 30–34]. MATLAB software (MATLAB R2013a, MathWorks, MA, USA) is used for computing all the parameters (PC scores, Mahalanobis distances and ROC).

Results and discussion

Fluorescence spectra of buccal mucosa, lateral, and dorsal surface of the tongue of oral cavity

Area normalized averaged fluorescence spectra recorded from buccal mucosa (BM), lateral border of tongue (LBT), and dorsal surface of tongue (DBT) of oral cavity to OSCC,

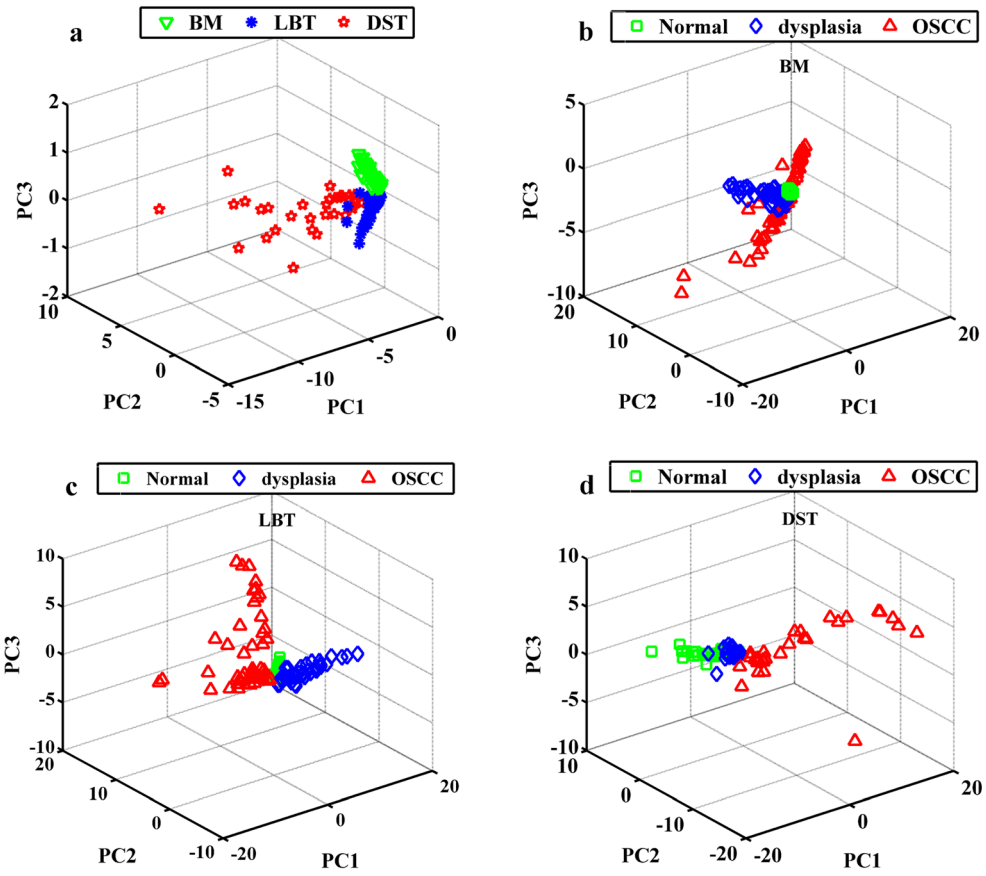

Fig. 4 Scatter plot of three PC scores (PC1, PC2, and PC3) obtained from fluorescence spectra of **a** normal tissue of three oral sites and different oral sites of normal, dysplasia, and OSCC groups **b** BM, **c** LBT, and **d** DST

dysplastic, and control groups at excitation wavelength 405 nm in the scan range of 450.14–763.41 nm are shown in Fig. 3a–c respectively. Number of sites involved in average spectra are summarized in Table 2. Major and minor bands of fluorescence spectra are seen in Fig. 3a–c. The green band around 500 nm is attributed to FAD and the red bands around 634, 676, 689, and 703 nm are due to endogenous porphyrins. In the typical spectra shown in Fig. 3e, bands 676 and 689 nm can be seen distinct. Though all bands of OSCC and dysplastic groups show differences in intensity from normal, differences in the 634 nm band are significant. Porphyrin contribution varies in the different sites, especially in the control group as shown in Fig. 3a–c respectively. Two minor porphyrin bands at 634 and 676 nm are noticed in 2 of the 36 volunteers of BM, 634, 676, and 689 nm bands of LBT in 7 of the 36 volunteers and 634, 676, 689, and 703 nm bands of DST in most of the volunteers. Some of the volunteers displayed dominant 634 nm bands and in some 676 and 689 nm bands were also visible which may be due bacterial infections. Typical spectra of a volunteer taken from different oral sites such as BM, soft palate (SP), retromolar trigone (RMT), LBT, DST, and lower lip (LL) are presented in Fig. 3d. Some oral sites such as RMT and BM show almost similar spectral profiles. LBT show weak porphyrin bands near 634 and 676 nm while DST show strong porphyrin bands. Among the above oral sites, SP have shown maximum fluorescence intensity. In Fig. 3e, typical spectra of two 47-year-old patients (OSCC and dysplastic) and a normal volunteer are plotted to show that porphyrin production does not appear to be an age related. Figure 3f shows typical spectra of a cancerous patient (addicted to cigarette, bidi, tobacco), a habitual (consuming tobacco 5 to 6 times and masala 2 to 3 times in a day for the last 10 years) and an inhabitual (consuming tobacco and masala 1 to 2 times in a day for the last 4 years) volunteer. As seen in Fig. 3f, habitual normal volunteer spectrum exhibits a few weak porphyrin features, not seen in inhabitual normal spectrum. However, the cancerous habitual shows further enhancement in the porphyrin peak as compared to habitual normal volunteer. This eliminates the doubt of porphyrin peaks being produced due to the bad habits. In the habitual normal, out of the eight volunteers, only five have shown changes in spectra while in the inhabitual normal, no changes are found in all nine volunteers.

Statistical analysis (PCA, Mahalanobis, and ROC)

PCA has been applied on the data sets of fluorescence spectra on different oral sites (BM, LBT, and DST) in the range 450.14 to 763.41 nm having dimension of 681. First 11 PCs (PC1 to PC11) consisting of an approximate variance of 99% have been chosen. Figure 4a displays a scatter plot of the first three PC scores (PC1, PC2, and PC3) of all three oral sites BM, LBT, and DST which

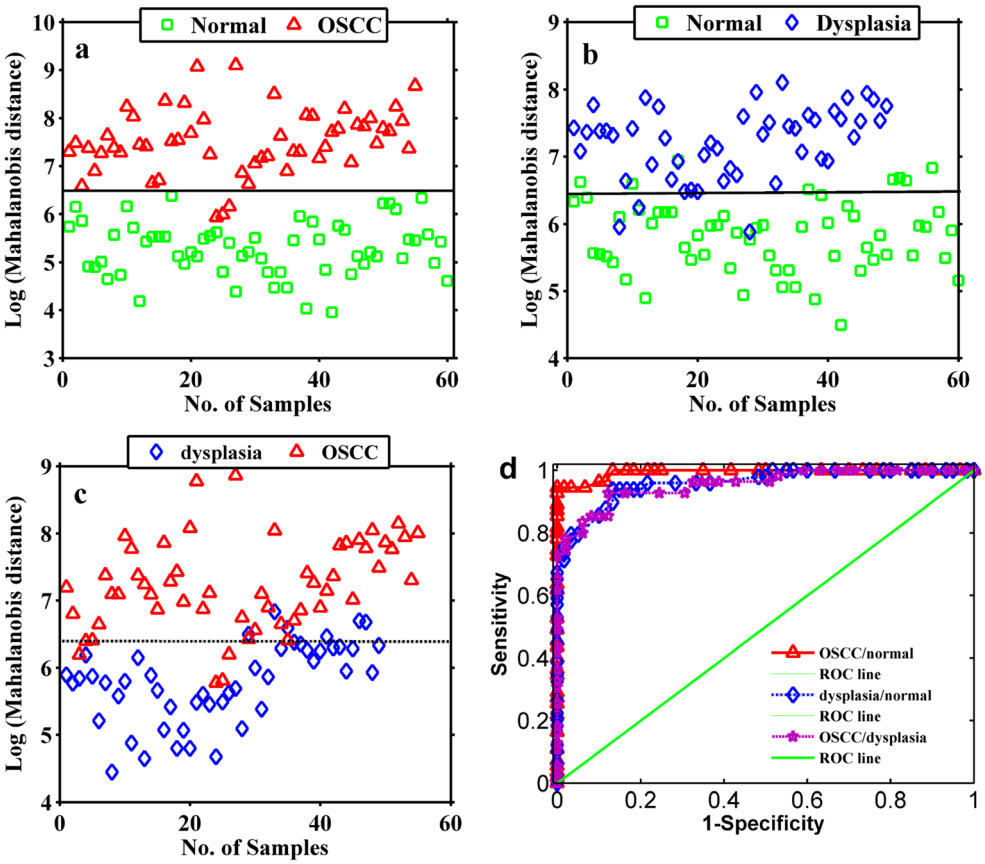

Fig. 5 Scatter plots of the Mahalanobis distance of LBT among the groups and ROC curves for **a** OSCC to normal, **b** dysplasia to normal, **c** OSCC to dysplasia, and **d** ROC curves

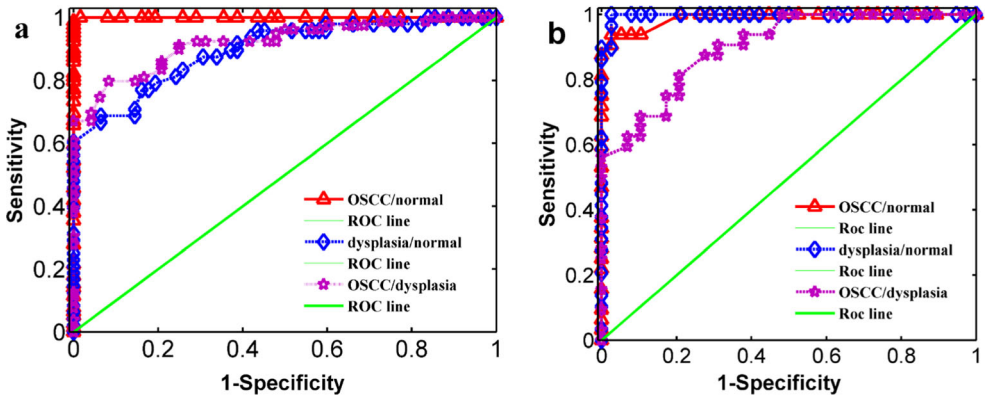

Fig. 6 ROC curves of OSCC to normal, dysplasia to normal, and OSCC to dysplasia for oral sites **a** buccal mucosa and **b** dorsal surface of tongue

consist of an approximate variance of 91%. One notices that clusters of each site are separated from one another with some overlap. It also signifies that there are spectral differences in the anatomic sites. In Fig. 4b–d, first three PC scores of all the three groups (normal, dysplastic, and OSCC) for oral sites BM, LBT, and DST respectively are shown. These three PC scores capture an approximate variance of 86% and show overlap among the groups. Clusters formed by normal group are localized in a small region compared to OSCC and dysplastic groups because of minor spectral differences.

PC scores of fluorescence spectra for each oral site are taken and loaded to Mahalanobis distance model one by one. Prior to calculate Mahalanobis distance for the groups, data sets of PC scores for each group are divided into training and validation sets respectively. Half of the data are taken as a training set and other half as validation set respectively. Mahalanobis distances of validation set data sets points are calculated from the mean of training set data points for each of the groups. Figure 5a–c show scatter plots of Mahalanobis distances (distance from OSCC to normal, distance from dysplasia to normal, distance from OSCC to dysplasia and vice versa) for LBT which are plotted against number of samples (patients/volunteers). ROC applied on these binary data sets differentiates the groups (OSCC to normal, dysplasia to normal, and OSCC to dysplasia) with sensitivities 94.55%, 93.88%, 92.73%, and specificities 100%, 86.67%, 87.76% with the overall accuracy of 99.33%, 95.77%, and 95.47% respectively.

ROC on binary date sets of Mahalanobis distances of BM differentiate the groups with sensitivities 98.73%, 71%, 79.15% and specificities 100%, 93.55%, 91.67% with the overall accuracy of 99%, 89.62%, and 91.98% respectively. Similarly ROC on the data set of DST differentiate the respective groups with sensitivities and specificities of 93.75%, 100%, 81.25% and 97.35%, 97.37%, 79.31% with the overall accuracy of 98.87%, 99.73%, and 90% respectively. ROC curves of LBT, BM and DST are shown in Fig. 5d and Fig. 6a and b respectively. Positive predictive value (PPV), negative predictive value (NPV), and accuracy have also been calculated and have been summarized in Table 3. It may be noted that the process of selecting training and validation data sets have been repeated several times by randomly selecting the data sets with no significant changes observed in sensitivities and specificities values.

Conclusion

This study involved an extensive comparison of fluorescence from different anatomical sites of oral cavity using an in-house-developed handheld probe. In vivo detection was based on two major fluorophores FAD and porphyrin in OSCC, dysplastic and normal groups. The red porphyrin fluorescence dominated in OSCC and dysplastic patients though it was also observed in the control group, particularly in the dorsal surface of tongue. Site-based classification was found to be important, because different locations of oral mucosa had shown differences in spectral profile due to difference in hardness and softness, skin colors, etc. Classification was performed by employing PCA, Mahalanobis distance model, and ROC. Oral sites LBT and DST displayed better discrimination than the BM, especially while discriminating precancer to normal. This may be due to the spread of the lesion (precancerous)

Table 3 PPV, NPV for LBT, BM, and DST of oral cavity among OSCC, dysplastic, and control groups

Sample type/oral sites	LBT		BM		DST	
	PPV (%)	NPV (%)	PPV (%)	NPV (%)	PPV (%)	NPV (%)
OSCC/normal	100	95	100	98	97	95
Dysplasia/normal	85	94	89.47	81	97	100
OSCC/dysplasia	89	91	94	73	81	79

Sensitivity = true positive(TP)/(TP + false negative(FN)); specificity = true negative(TN)/(TN + false positive(FP)); PPV = TP/(TP+FP); NPV = TN/(TN+FN), accuracy = (TP+TN)/((TP+FP+FN+TN)

over a wide region, with inhomogeneity in the case of BM, while the lesion of other two sites (LBT and DST) were more localized. In conclusion, the handheld probe combined with a robust classification tool such as PCA and Mahalanobis may be useful as a screening tool for oral precancer.

Acknowledgements We would like to acknowledge IMPRINT India, MHRD government, for the financial support.

Compliance with ethical standards

Conflict of interest statement The authors declare that they have no conflicts of interest.

Role of funding source Facilities of Biophotonics lab at IIT Kanpur has been utilized in the study.

Ethics approval The study was approved by the Ethics Committee of GSVM Medical College Kanpur and IIT Kanpur and performed in accordance with the Declaration of Helsinki.

Informed consent Informed consent form was taken from all participating patients and volunteers.

Publisher's note Springer Nature remains neutral with regard to jurisdictional claims in published maps and institutional affiliations.

References

1. Omar E (2015) Current concepts and future of noninvasive procedures for diagnosing oral squamous cell carcinoma–a systematic review. Head Face Med 11: 6
2. Varshitha A (2015) Prevalence of oral cancer in India. J Pharm Sci Res 7:845–848
3. Thomas J, Vineet DA, Rasheena PM, Krishnan JK (2013) Early detection of precancerous and cancerous lesions: an overview. JIAOMR 25:35–39
4. Yardimci G, Kutlubay Z, Engin B, Tuzun Y (2014) Precancer lesions of oral mucosa. World J Clin Cases 2:866–872
5. Dikshit R, Gupta PC, Ramasundarahettige C, Gajalakshmi V, Aleksandrowicz L, Badwe R, Kumar R, Roy S, Suraweera W, Bray F, Mallath M, Singh PK, Sinha DN, Shet AS, Gelband H, Jha P, Million Death Study Collaborators (2012) Cancer mortality in India: a nationally representative survey. Lancet 379:1807–1816
6. Scully C, Bagan JV, Hopper C, Epstein JB (2008) Oral cancer: current and future diagnostic techniques. Am J Dent 21:199–209
7. Koenig K, Schneckenburger H (1994) Laser-induced autofluorescence for medical diagnosis. J Fluoresc 4:17–40
8. de Oliveira Silva FR, Bellini MH, Tristão VR, Schor N, Vieira ND Jr, Courrol LC (2010) Intrinsic fluorescence of protoporphyrin IX from blood samples can yield information on the growth of prostate tumours. J Fluoresc 20:1159–1165
9. Inaguma M, Hashimoto K (1999) Porphyrin-like fluorescence in oral cancer: in vivo fluorescence spectral characterization of lesions by use of a near-ultraviolet excited autofluorescence diagnosis system and separation of fluorescent extracts by capillary electrophoresis. Cancer 86:2201–2211
10. Alfano R, Tang G, Pradhan A, Lam W, Choy D, Opher E (1987) Fluorescence spectra from cancerous and normal human breast and lung tissues. IEEE J Quantum Electron 23:1806–1811
11. Alfano R, Yang Y (2003) Stokes shift emission spectroscopy of human tissue and key biomolecules. IEEE J Sel Top Quantum Electron 9:148–153
12. Ramanujam N, Mitchell MF, Mahadevan-Jansen A, Thomson SL, Staerkel G, Malpica A, Wright T, Atkinson N, Richardas-Kortum R (1996) Cervical precancer detection using a multivariate statistical algorithm based on laser-induced fluorescence spectra at multiple excitation wavelengths. Photochem Photobiol 64:720–735
13. de Veld DC, Bakker Schut TC, Skurichina M, Witjes MJ, Van der Wal JE, Roodenburg JL, Sterenborg HJ (2005) Autofluorescence and Raman microspectroscopy of tissue sections of oral lesions. Lasers Med Sci 19:203–209
14. Hillemanns P, Reiff J, Stepp H, Soergel P (2007) Lymph node metastasis detection of ovarian cancer by porphyrin fluorescence photodetection: case report. Lasers Med Sci 22:131–135
15. Devi S, Panigrahi PK, Pradhan A (2014) Detecting cervical cancer progression through extracted intrinsic fluorescence and principal component analysis. J Biomed Opt 19:127003
16. Bergholt MS, Zheng W, Lin K, Ho KY, Teh M, Yeoh KG, So JB, Huang Z (2011) Combining near-infrared-excited autofluorescence and Raman spectroscopy improves in vivo diagnosis of gastric cancer. Biosens Bioelectron 26:4104–4110
17. Tromberg BJ, Shah N, Lanning R, Cerussi A, Espinoza J, Pham T, Svaasand L, Butler J (2000) Non-invasive in vivo characterization of breast tumours using photo migration spectroscopy. Neoplasia 2: 26–40
18. Farwell DG, Meier JD, Park J, Sun Y, Coffman H, Poirier B, Phipps J, Tinling S, Enepekides DJ, Marcu L (2010) Time- resolved fluorescence spectroscopy as a diagnostic technique of oral carcinoma. Arch Otolaryngol Head Neck Surg 136:126–133
19. Amelink A, Sterenborg HJ, Roodenburg JL, Witjes MJ (2011) Noninvasive measurement of the microvascular properties of non-dysplastic and dysplastic oral leukoplakias by use of optical spectroscopy. Oral Oncol 47:1165–1170
20. Singh SP, Deshmukh A, Chaturvedi P, Murali KC (2012) In vivo Raman spectroscopic identification of premalignant lesions in oral buccal mucosa. J Biomed Opt 17:105002
21. Pichardo-Molina JL, Frausto-Reyes C, Barbosa-García O, Huerta-Franco R, González-Trujillo JL, Ramírez-Alvarado CA, Gutiérrez-Juárez G, Medina-Gutiérrez C (2007) Raman spectroscopy and multivariate analysis of serum samples from breast cancer patients. Lasers Med Sci 22:229–236
22. Yuvaraj M, Aruna P, Koteeswaran D, Tamilkumar P, Ganesh S (2015) Rapid fluorescence spectroscopic characterization of salivary DNA of normal subjects and OSCC patients using ethidium bromide. J Fluoresc 25:79–85
23. Kumar P, Singh A, Kumar Kanaujia S, Pradhan A (2018) Human saliva for oral precancer detection: a comparison of fluorescence and Stoke shift spectroscopy. J Fluoresc 28:419–426
24. Gillenwater A, Jacob R, Ganeshappa R, Kemp B, El-Naggar AK, Palmer JL, Clayman G, Mitchell MF, Richarda_Kortum R (1998) Noninvasive diagnosis of oral neoplasia based on fluorescence spectroscopy and native tissue autofluorescence. Arch Otolaryngol Head Neck Surg 124:1251–1258
25. Majumder SK, Mahanty SK, Ghosh N, Gupta PK, Jain DK, Khan F (2000) A pilot study on the use of autofluorescence for diagnosis of the cancer of human oral cavity. Curr Sci 79:1089–1094
26. Lane PM, Gilhuly T, Whitehead P, Zeng H, Poh CF, Ng S, Williams PM, Zhang L, Rosin MP, MacAulay CE (2006) Simple device for the direct visualization of oral-cavity tissue fluorescence. J Biomed Opt 11:024006
27. De Veld DC, Sterenborg HJ, Roodenburg JL, Witjes MJ (2004) Effect of individual characteristics on healthy oral mucosa autofluorescence spectra. Oral Oncol 40:815–823
28. Jayanthi JL, Subhash N, Stephen M, Philip EK, Beena VT (2011) Comparative evaluation of the diagnostic performance of

autofluorescence and diffuse reflectance in oral cancer detection: a clinical study. J Biophotonics 4:696–706
29. Nazeer SS, Asish R, Venugopal C, Anita B, Gupta AK, Jayasree RS (2014) Noninvasive assessment of the risk of tobacco abuse in oral mucosa using fluorescence spectroscopy: a clinical approach. J Biomed Opt 19:057013
30. Abdi H, Williams LJ (2010) Principal component analysis. Wiley Interdiscp Rev: Comput Stat 2:433–459
31. De Maesschalac R, Jouan-Rimbaud D, Massart DL (2000) The Mahalanobis distance. Chemom Intell Lab Syst 50:1–18
32. Brereton RG (2015) The Mahalanobis distance and its relationship to principal component scores. J Chemom 29:143–145
33. Fawcett T (2006) An introduction to ROC analysis. Pattern Recogn Lett 27:861–874
34. Akobeng AK (2007) Understanding diagnostic test 3: receiver operating characteristic curves. Acta Paediatr 90:644–647